

## Declines in global ecological security under climate change

Jianping Huang<sup>a,b,\*</sup>, Haipeng Yu<sup>c</sup>, Dongliang Han<sup>b</sup>, Guolong Zhang<sup>b</sup>, Yun Wei<sup>b</sup>, Jiping Huang<sup>d</sup>, Linli An<sup>b</sup>, Xiaoyue Liu<sup>b</sup>, Yu Ren<sup>b</sup>

<sup>a</sup> Collaborative Innovation Center for Western Ecological Safety, Lanzhou University, Lanzhou 730000, China

<sup>b</sup> College of Atmospheric Sciences, Lanzhou University, Lanzhou 730000, China

<sup>c</sup> Key Laboratory of Land Surface Process and Climate Change in Cold and Arid Regions, Northwest Institute of Eco-Environment and Resource, Chinese Academy of Sciences, Lanzhou 730000, China

<sup>d</sup> Enlightening Bioscience Research Center, Mississauga L4X 2X7, Canada



### ARTICLE INFO

#### Keywords:

Ecological security  
Oxygen cycle  
Climate change  
Index

### ABSTRACT

Ecological security is the state when an ecosystem maintains its stability under external stress. Due to climate change and the increase in human activities since the 20th century, the rapid decline in global ecological security has threatened sustainable human development. The evaluation and projection of global ecological security is important for forming adaptation strategies to maintain sustainable development in sensitive areas. However, the current assessments of ecological security mainly focus on regional scales, and the interactions among different factors have not been considered, resulting in future projections having substantial uncertainty. Here, a new index of ecological security was developed by including biological, oxygen, carbon, thermal and hydrological cycles and the impacts to ecosystem stability from climate change and human activities at a global scale. A global distribution map of ecological security has been established that covers the past 60 years and includes projections for the future 100 years. A severe decline in ecological security has occurred in drylands that has expanded into surrounding regions over the past 60 years. The response of ecological security to global warming and human activities is projected to be stronger. By ~2100, under a high greenhouse gas emissions scenario, the amount of globally insecure land would cover more than 57% of the land in the world.

### 1. Introduction

Ecological security refers to a state in which natural and semi-natural ecosystems can maintain stability, associated with the ecological environment provides ecological guarantees for the sustainable development of the whole eco-economic system (Costanza and Mageau, 1999; Fu, 2010; Ma et al., 2004; Rapport, 1989; IUCN, 2012; Jenkins et al., 2013; Newbold et al., 2015). However, ecological security has been severely threatened under on-going global warming and enhanced human activities (Walther et al., 2002; Palmer et al., 2004; Piao et al., 2010; Huang et al., 2012, 2015, 2016; Feng et al., 2016; Fu et al., 2017; Zhao et al., 2018). There are some studies indicating that ecological destruction has caused desertification, food shortages (Glover et al., 2010) and water insecurity (Vörösmarty et al., 2010; Humphrey et al., 2017), which will threaten human survival and development in the 21st century. Ecological security is closely associated with biological, oxygen, carbon, hydrological and thermal cycles under climate change and human activities. This is because, changes in vegetation structure and function linked to oxygen cycle, controls the exchange of carbon,

water and energy between the land and the atmosphere (Piao et al., 2020). However, the consequences of these transformations for ecological security are poorly understood. Understanding the change in these indicators is important to determining terrestrial ecological security through the processes of respiration, photosynthesis and burning. Hence, knowledge of how climate change and human activities will affect changes in ecological security in the future is essential for protection and for adaptation strategies.

Though the concept of ecological security has been proposed as early as the 1970s (Sohn, 1973), a unified and generally accepted definition has not been formed because ecological security is a complex issue that involves many aspects (Daly, 2005; Hodson & Marvin, 2009; Wang et al., 2015; Feng et al., 2018). There are two limitations to the current assessment of ecological security. First, in previous studies (Hodson & Marvin, 2009; Wang et al., 2015; Feng et al., 2018), although some indicators have been used to evaluate regional ecological security, those assessments have only considered individual regional issues, such as water security (Shinoda and Yamaguchi, 2003; Sorooshian et al., 2005; Seneviratne et al., 2010; Wang et al., 2015) and

\* Corresponding author at: Collaborative Innovation Center for Western Ecological Safety, Lanzhou University, Lanzhou 730000, China.

E-mail address: [hjp@lzu.edu.cn](mailto:hjp@lzu.edu.cn) (J. Huang).

<https://doi.org/10.1016/j.ecolind.2020.106651>

Received 20 April 2020; Received in revised form 14 June 2020; Accepted 21 June 2020

Available online 01 July 2020

1470-160X/ © 2020 Elsevier Ltd. All rights reserved.

urban ecological security (Hodson & Marvin, 2009). Second, as ecological security has various definitions (Allenby 2000; Liu & Chang, 2015; Hu et al., 2019), there has been no uniform and well-recognized indicator system. Therefore, it is important to understand how the variability on climate change and human activities constrains biological, oxygen, carbon, hydrological and thermal cycles to determine the ecological security.

In fact, ecological security involves various cycles in an ecosystem. The oxygen, carbon, hydrological and thermal cycles are interconnected throughout all regions on Earth, and they are also coupled to all biological cycles (Schlesinger et al., 1990; Ciais, 1999; Jacobson et al., 2000; Dickinson, 2005; Fu & Li, 2016; Huang et al., 2017a,b, 2018; Yang et al., 2019). The process of photosynthesis not only produces vital O<sub>2</sub> and is important for the food chain but also absorbs solar irradiation and carbon balance. Carbon accumulates in soils in large quantities, major because the high water levels that result in low biological activity and slow soil organic carbon decomposition. Carbon accumulation plays an important driving role in the carbon cycle through atmosphere, green vegetation and surface soils. Thus, these factors are the most important ecological indicator for changes in biological, oxygen, carbon, hydrological and thermal cycles. The ecological security means the survival of humans and other animals should be balanced with plant vegetation within the above five cycles. Here, the aim of this study is to establish a framework for considering the interaction among biological, oxygen, carbon, thermal and hydrological cycles and to propose a quantitative evaluation to measure ecological security over global land and project its future changes. We address the following questions: (1) How to identify and measure ecological security and establish the global grid datasets of global ecological security (2) How to project the future changes of global ecological security.

## 2. Data compilation

In this study, the ecological security is identified by the combination of four essential factors, including oxygen consumption (O<sub>c</sub>), oxygen production (O<sub>p</sub>), temperature warming magnification (T<sub>m</sub>) and the aridity index (AI). The data compilation of each term are described below.

### 2.1. Oxygen consumption

O<sub>2</sub> is consumed by a wide range of processes, some of which are negligible or are difficult to quantify, including the weathering of organic matter and sulfide minerals, volcanic gas oxidation and so on. In this paper, five main O<sub>2</sub> consumption processes, including (1) fossil fuel combustion, (2) human respiration, (3) livestock respiration, (4) fires and (5) heterotrophic and soil respiration, are considered (Petsch, 2013). The detailed methods and datasets of the processes (1)-(4) could be found in Huang et al. (2018) and Liu et al., (2020). Here, the heterotrophic and soil respiration (R<sub>h</sub> + R<sub>d</sub>) is the process that consumes oxygen when soil organisms respire, where R<sub>h</sub> is the respiration by heterotrophs and R<sub>d</sub> is the respiration by decomposers (microbes), which is measured by the difference between net primary productivity (NPP) and net ecosystem productivity (NEP). The simulated R<sub>h</sub> + R<sub>d</sub> dataset (see Table 1) is obtained from the simulation of the Fifth Coupled Model Intercomparison Project (CMIP5) (Taylor et al., 2012). The observed R<sub>h</sub> + R<sub>d</sub> data are obtained from the Global Fire Emissions

Database (GFED, <http://www.globalfiredata.org>, Van et al., 2017).

### 2.2. Oxygen production

Oxygen is produced during photosynthesis, during which plants and other organisms absorb carbon dioxide (CO<sub>2</sub>) from the atmosphere and release oxygen (O<sub>2</sub>). Photosynthesis can be expressed by the following chemical equation:



Gross primary production (GPP) is the total amount of CO<sub>2</sub> fixed by a plant during photosynthesis. NPP is the net amount of gross primary productivity remaining after including the cost of plant respiration. According to Eq. (1), we can use the following equation to calculate the net amount of O<sub>2</sub> produced during the process of photosynthesis if the known amount of carbon is fixed through photosynthesis (NPP).

$$\text{O}_2 = \text{NPP} \times 2.667 \quad (2)$$

Due to the molar mass of O<sub>2</sub> is 32 g per mole and the C is 12 g per mole, thus the ratio is 2.667. The simulated NPP dataset from 1948 to 2100 is obtained from the CMIP5 simulation (Taylor et al., 2012) and the observed NPP data based on MODIS from 2000 to 2015 were acquired from the Global Fire Emissions Database (Van et al., 2017). The simulated NPP and observed NPP data are re-gridded to a 1.0° × 1.0° resolution for comparison. The detailed methods and datasets of oxygen production could be found in Huang et al. (2018) and Liu et al. (2020).

### 2.3. Temperature warming magnification

The temperature warming magnification is represented by T<sub>m</sub>(i,n), which is defined as the ratio of the grid warming rate to the global warming rate and as follows:

$$T_m(i, n) = \frac{T_{trend}(i, n)}{T_{Gtrend}(n)} \quad (3)$$

where T<sub>trend</sub>(i,n) is defined as the linear trend of the surface temperature from 1901 to year n at grid point i, and T<sub>Gtrend</sub>(n) is defined as the linear trend of the global average surface temperature from 1901 to year n for year n.

The CRUTEMP4 dataset, which is developed by the Met Office Hadley Centre and the Climatic Research Unit at the University of East Anglia (Morice et al., 2012), combines both surface air (over land) and sea surface (over ocean) temperature data. To fill the missing values in the CRUTEMP4, Dai and Zhao (2017) have supplemented the CRUTEMP4 with CRU TS2.3 temperature data. Therefore, we use this modified version of the CRUTEMP4 to calculate observed T<sub>Gtrend</sub> and T<sub>trend</sub>. For simulations, the surface air temperature data used to calculate T<sub>Gtrend</sub> and T<sub>trend</sub> are obtained from 20 CMIP5 climate models (Taylor et al., 2012). We averaged the T<sub>m</sub> data of 20 models to calculate the ecological security index (ESI) for each model (see Table 1).

### 2.4. Aridity index

The AI (i,n) represents the aridity index at grid i for year n, which is defined as the ratio of precipitation to potential evapotranspiration (PET) and denoted as

**Table 1**  
Details of CMIP5 models used in this study.

Variables	Model member
NPP	CanESM2, CCSM4, GFDL-ESM2G, GFDL-ESM2M, HadGEM2-CC, HadGEM2-ES, MIROC-ESM, MIROC-ESM-CHEM, NorESM1-M
R <sub>h</sub> + R <sub>d</sub>	
T <sub>m</sub>	BCC-CSM1.1, CanESM2, CCSM, CNRM-CM5, CSIRO-Mk3.6, GFDL-CM3, GFDL-ESM2G, GFDL-ESM2M, GISS-ER, HadGEM2-CC, HadGEM2-ES, INMCM4, IPSL-CM5A-LR, IPSL-CM5A-MR, MIROC5, MIROC-ESM, MIROC-ESM-CHEM, MPI-ESM-LR, MRI-CGCM3, NorESM1-M
AI	

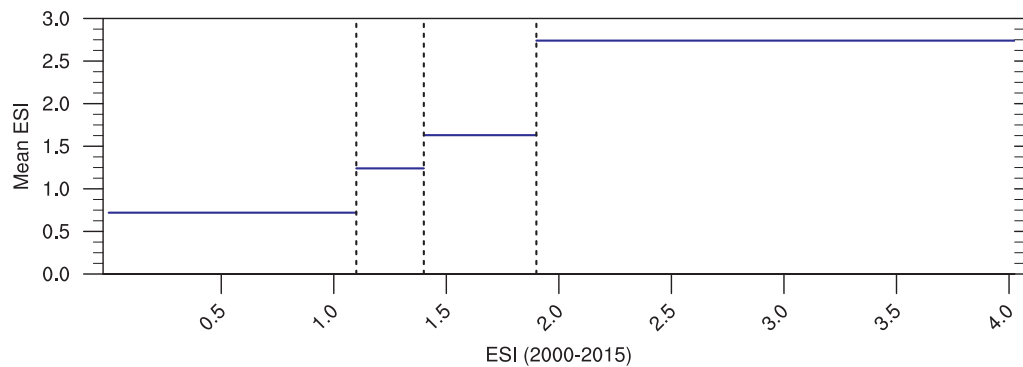


Fig. 1. The average value of the mean ESI during the period 2000–2015 under each classification. The abscissas corresponding to the dotted lines are the hierarchical intervals.

$$AI(i, n) = \frac{P(i, n)}{PET(i, n)} \tag{4}$$

For observation, the precipitation data is from the NOAA’s PRECipitation REConstruction over Land (PREC/L) dataset (Chen et al., 2002) developed by the Climatic Prediction Center (CPC), which covers for 1948 to the present on a 0.5° grid. And the PET data is from CRU TS 3.25 dataset (Harris et al., 2014), which covers the period 1901–2016 and all land areas at 0.5° resolution. In order to be consistent with the AI in the models, we keep the climatology of observed precipitation and PET data consistent with the observed precipitation and PET data provided by Feng and Fu (2013).

For simulations, the precipitation and PET simulation datasets used here are provided by Feng and Fu (2013). These data are derived from the monthly mean temperature, precipitation, solar radiation, specific humidity and wind speed products obtained from the CMIP5 climate models (Taylor et al., 2012). Feng and Fu (2013) provided AI data from 20 models, which are not consistent with the models that can provide NPP and Rh + Rd. Therefore, we averaged the AI data of 20 models to calculate the ESI for each model (Table 1).

### 2.5. Land datasets

The surface energy flux data for sensible and latent heat, 0–7 cm volumetric soil water, and 0–7 cm soil temperature data were collected from the ERA5 reanalysis from the European Centre for Medium-Range Weather Forecasts (ECMWF) on a 0.25° × 0.25° grid for 2000 to 2015. In addition, for verification, we used the CPC Soil Moisture dataset (Fan and Dool, 2014) on a 0.5° × 0.5° grid from a model, which covers the period of 1948-present and was provided by the NOAA/OAR/ESRL PSD, Boulder, Colorado, USA, and we also explored the surface energy flux data for sensible and latent heat, and 0–10 cm soil moisture content from the NASA Global Land Data Assimilation System (GLDAS) land model simulation using the Noah Land Surface Model forced by observational data on a 1° × 1° grid (GLDAS\_NOAH10\_M.2.0) for 1948 to 2010.

### 3. Ecological security measurements

As the land was disrupted by human activities and climate change, here biological, oxygen, carbon, thermal and hydrological cycles were considered to assess ecological security of global land. Here, an ESI is defined to identify and measure the security state of global ecological system and project the coming change of insecure land. By combing four terms described in section 2.1, the ESI is constructed as follows:

$$ESI = \left( \frac{O_c}{O_p} \cdot T_m \cdot \frac{1}{AI} \right)^{\frac{1}{3}} \times 10 \tag{5}$$

here, ESI is an interconnected multi-disciplinary indicator for

describing the stability state of terrestrial ecosystem, which includes the human-induced oxygen consumptions, vegetation photosynthesis, precipitation, potential evapotranspiration and temperature. Here the oxygen-related parameters are used to indicated the ecosystem activity. Besides, the vulnerability of ecosystem would be highly impacted by the stresses on ecosystem. Temperature warming and aridity change would impact local ecological security. Therefore, we assess land ecological security under climate change and human activities by integrating the oxygen-related parameters, AI and temperature magnification.

To eliminate the effects of extreme values, we set the 1% and 99% thresholds as the minimum and maximum values to normalize  $O_c/O_p$ ,  $T_m$  and  $1/AI$ , then each term was limited to between 0 and 1. Next, the ESI was defined by aggregating the three terms by Eq.1. Hence, the value of the ESI is limited to the range 0–10. For model simulations, to focus on the temporal variation and long-term climate change, the model simulations are adjusted to have the same mean normalized  $O_c/O_p$ ,  $T_m$  and  $1/AI$  of 2000–2015 as the observations.

We assumed that there was a significant difference between the ESI indices at each classification, and the ESI values in each classification should have one aggregation center. After that, the probability density distribution of the ESI should have several peaks. We use the ESI value corresponding to the valley of the probability density distribution as the threshold of the classification. Based on these norms, we used the values corresponding to the three valleys of the probability density distribution of ESI as the classification thresholds, which are 1.1, 1.4 and 1.9, respectively. In addition, the difference from other hierarchical aggregation centers is the most significant. Fig. 1 shows the average value in each classification for the mean ESI during the period 2000–2015. The mean values of ESI for secure, semi-secure, light-dangerous and severe-dangerous regions are 0.72, 1.24, 1.63 and 2.74, respectively. The difference of ESI between various classification passed the significance test at 99% level. So, ESI is divided into four levels with thresholds of 1.1, 1.4 and 1.9, respectively. Insecure land is defined as a region with  $ESI \geq 1.1$ , which can be further divided into the subtypes of severe-dangerous ( $ESI \geq 1.9$ ), light- dangerous ( $1.4 \leq ESI < 1.9$ ) and semi-secure ( $1.1 \leq ESI < 1.4$ ) regions. Secure land is defined as a region with  $ESI < 1.1$  here.

The declining of ecological security corresponds to the expansion of ecological insecure land. When land on Earth is short on water and loses the ability for plants to produce oxygen through photosynthesis, this land will invade and destroy the surrounding environment and gradually expand its territory to form more deserts or drylands on Earth, which results in a positive feedback cycle in which warming and drying reinforce each other (Fig. 2). We define this type of insecure land as natural insecure land. Meanwhile, the migration of populations has created more mega-cities and concentrated industrial districts, resulting in increasing demand for fresh water and loss of plants (Cai et al., 2015). These detrimental environmental effects can apparently influence and invade nearby areas if no actions are taken to compensate for

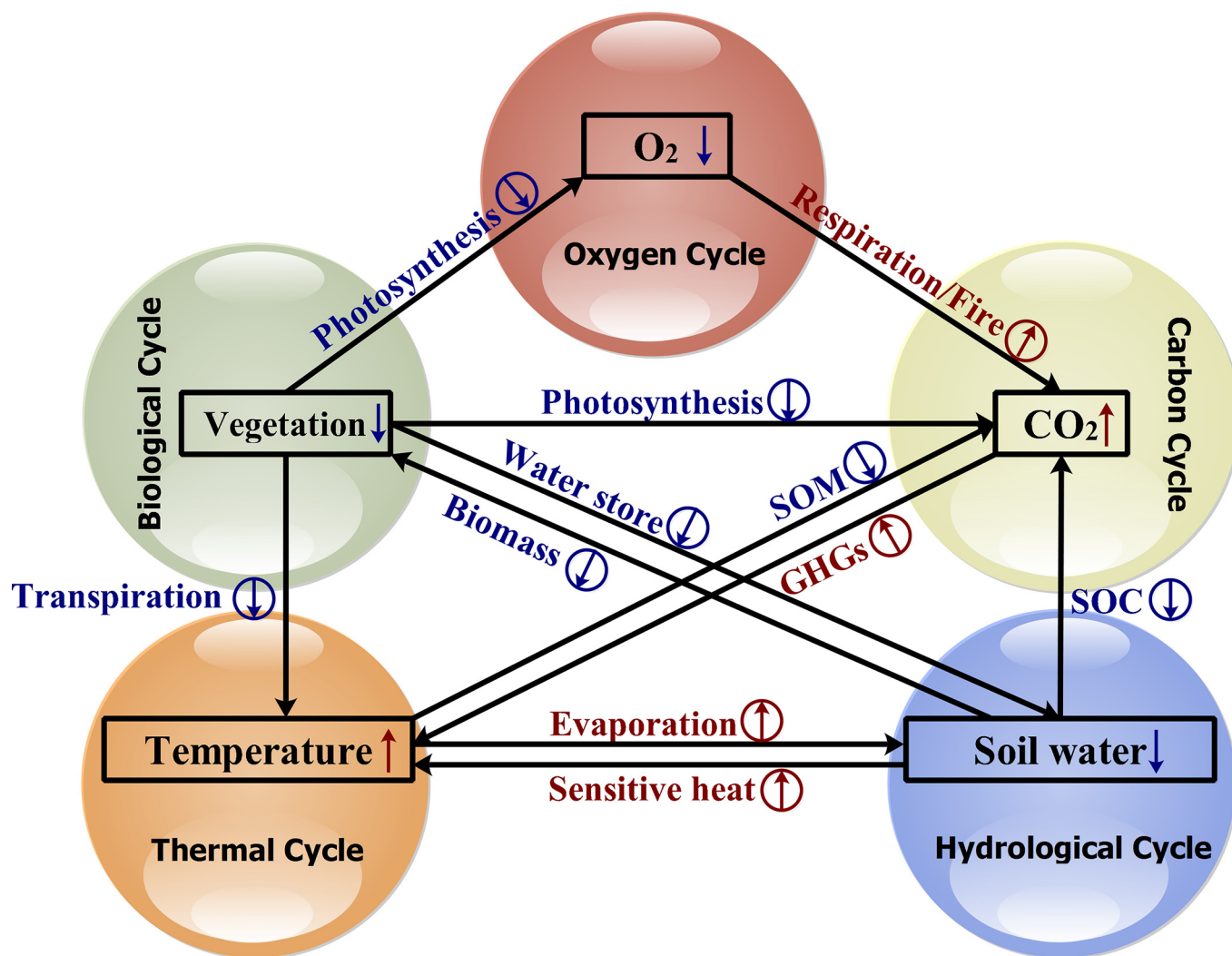


**Fig. 2.** Conceptual framework for ecological security index. The connections of indicators from oxygen cycle (oxygen production and consumption), biological cycle (vegetation photosynthesis and biomass), thermal cycle (soil temperature, evaporation and sensible heat flux), hydrological cycle (soil water and TWS) and carbon cycle (SOC and  $CO_2$ ) are described. The changes of indicators associated with symbols  $\downarrow$  (blue) or  $\uparrow$  (red) indicate the decrease and increase in response to ecological insecure land compared to the ecological secure land. The single arrows (black) represent the paths of indicators. The  $O_2$ ,  $CO_2$ , TWS and SOC indicate oxygen, carbon dioxide, terrestrial water storage and soil organic carbon, respectively.

and prevent them. We define these regional areas as anthropogenic insecure land. The total insecure land comprises the above mentioned natural and anthropogenic insecure lands. The more insecure land that grows, the less oxygen is produced along with the greater loss of fresh water and plants, resulting in less land that is suitable for supporting human life. Therefore, the key to maintaining secure land is to control the balance between the regional oxygen, water, carbon and thermal cycles; otherwise, adverse effects, including the release of heat and soil dust, will directly affect the ambient land through a vicious cycle (Fig. 2).

Based on the framework established above, the ESI is constructed with the terms in Eq.5 are closely associated with oxygen, carbon, soil, water and thermal cycles, which play indiscernible roles in global land ecosystems (Fig. 2).

#### 4. Results analysis

Fig. 3 shows the spatial distribution of ESI values determined by observations obtained between 60°S-60°N from 2000 to 2015. The area coverage of the insecure land represents 53.0% of the global land area (60°S-60°N), and the proportions of the different land surface types (60°S-60°N) of the semi-secure, light-dangerous and severe-dangerous

regions are 13.3%, 16.4% and 23.3%, respectively (Fig. 3b). Here, desert covers 15.9% of the global land, representing deserts such as Sahara and Taklimakan (Fig. 3a). The severe-dangerous regions are mainly distributed at the edges of deserts and regions highly affected by climate change and some other places with high human activities, including industrial and densely populated regions (Fig. 3a). The light-dangerous regions include some drylands and mountainous plateau regions without vegetation and snow cover (Fig. 3a), which are located in Australia, North America, Europe, southern Africa and Central Asia. The semi-secure regions are transition zones between secure and dangerous land, which are mainly distributed in semi-arid and cattle-producing regions (Fig. 3a), where the amount of oxygen generated via photosynthesis cannot compensate for the oxygen consumption. Only 31.2% of the global land area is covered by land that is defined as secure, which is mainly distributed in South America, Siberia, Central Africa and the Tibetan Plateau; these areas have strong ecological resilience and have not been disturbed by humans. In addition, the cryosphere (polar regions and Greenland), which is not discussed in this study, can also be classified as secure land that stores plenty of freshwater without human disturbances.

Based on the above climatology, it is essential to investigate how ecological security will change in the future. The CMIP5 has generated

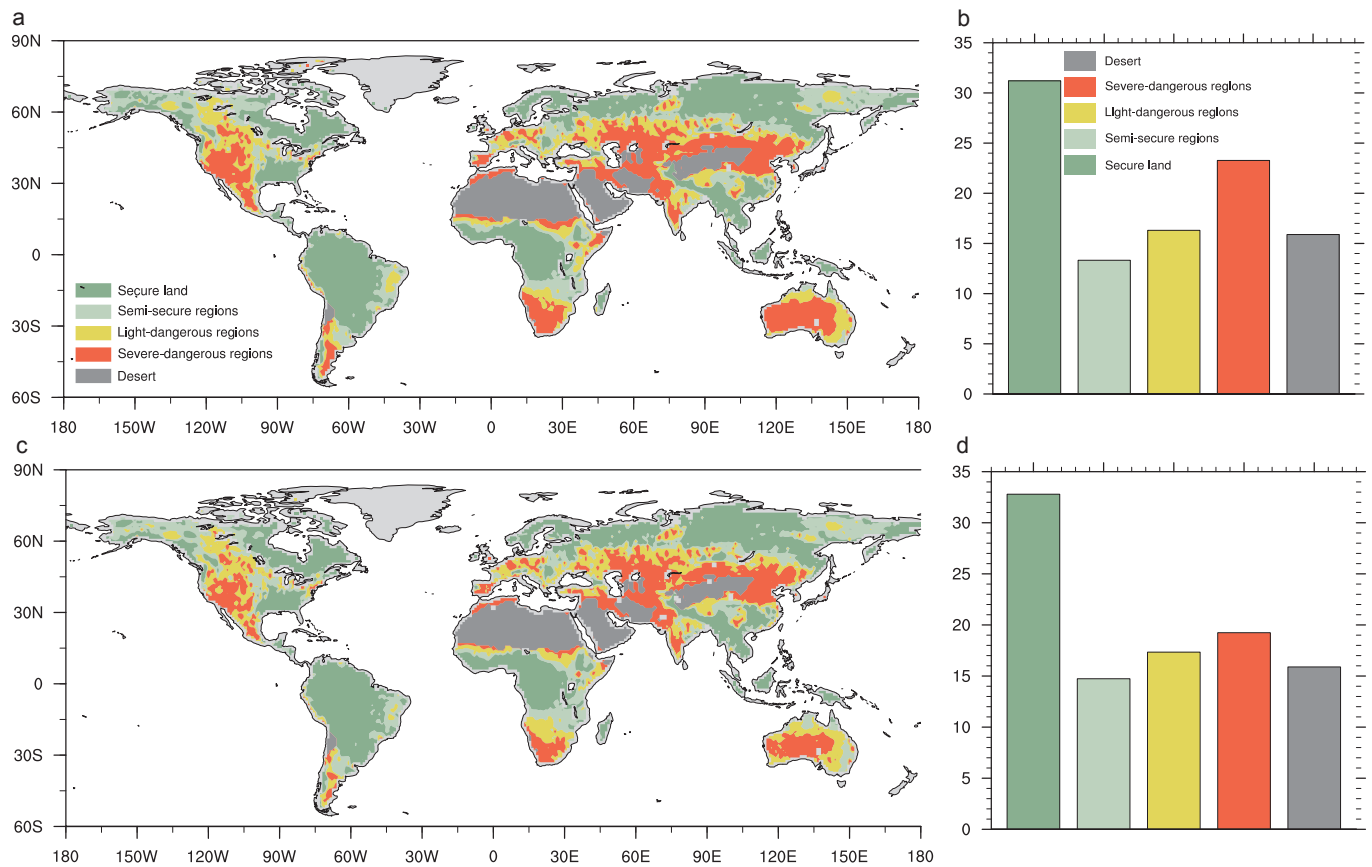


**Fig. 3.** Global distribution of ESI and area coverage of different land surface types based on observations (a–b) and CMIP5-EM (historical and RCP8.5) (c–d) from 2000 to 2015. a, Spatial distribution of observed ESI values for 2000–2015. b, Area coverage (percentage) of different land surface types (60°S–60°N) based on observed ESI values from 2000 to 2015. c and d are similar to a and b but for CMIP5-EM.

projections using several emissions scenarios and has provided a crucial reference for the spatial and temporal evolution of ecological security in the future. The model members used are shown in Table 1 and the ensemble mean of these CMIP5 models (CMIP5-EM), which filters the uncertainty from the inter-model variability and better reflects the changes in ESI, is used in this study. To ensure the reliability of future projections, the CMIP5-EM simulations of ESI over 2000–2015 (Fig. 3c–d) are compared to observations. The results show that the spatial distribution and the area coverage of insecure land obtained by CMIP5 are consistent with those indicated by observations, indicating that CMIP5 is adequate for projecting future ESI changes. For the CMIP5-EM historical and RCP8.5 simulated ESI values from 2000 to 2015, the area coverage of insecure land represents 51.2% of the global land area, and those of the different land surface types (60°S–60°N) of secure regions, semi-secure regions, light-dangerous regions and severe-dangerous regions are 32.8%, 14.7%, 17.3% and 19.2%, respectively. Desert covers 15.9% of the global land area, which is mainly located Sahara and Taklimakan; this result is similar to that indicated by observations (Fig. 3c–d). The light-dangerous and severe-dangerous regions are mainly distributed in the middle and high latitudes of the Northern Hemisphere, such as in western North America, Southwest Russia and Northeast China. Generally, the CMIP5 models can capture the spatial distribution of the ESI values from 2000 to 2015, indicating that the CMIP5-EM is adequate for projecting future changes in ESI.

Fig. 4a present the time series of the global mean ESI during the future periods. For future projections, the ESI increases to ~ 1.8 by ~ 2100 under RCP8.5 scenario and decreases from ~ 1.5 (~2020) to ~ 1.4 by 2100 under RCP4.5. These opposite trends demonstrate that the emission of greenhouse gases is the main factor controlling the variations in ESI and that the restriction of greenhouse gas emissions

under RCP4.5 could mitigate this disease. Fig. 4b–f presents the time series of the changes in area of the four subtypes during the historical and future periods. Clearly, the expansion of severe-dangerous regions in the future is significant under the RCP8.5 scenario. In addition, the area coverage of semi-secure and secure regions will decrease after 2005 under the RCP8.5 scenario. However, by reducing oxygen consumption through limiting carbon dioxide emissions under the RCP4.5 scenario, the global expansion of total insecure land will be inhibited. The area coverage of severe-dangerous regions will first increase and then decrease; simultaneously, the areas of secure regions will first decrease and then increase. Under the RCP4.5 scenario, the areas of the four land surface types at the end of the century will change little compared with those at the beginning of this century. Among them, the areas of severe-dangerous regions and light-dangerous regions will decrease slightly; conversely, the areas of secure regions will increase slightly.

Fig. 5 shows the spatial distribution of the mean ESI in 2085–2100 and the areal changes of insecure land indicated from RCP8.5 scenario by CMIP5-EM. By the end of this century, the area coverage of insecure land will be 57.1% of the global land area, which will mainly be distributed in Africa, India, Europe, West and East Asia, and the different land surface types (60°S–60°N) of secure regions and semi-secure regions will be 27.1% and 13.1%, respectively. Relative to the beginning of this century (Fig. 3), the area of secure, semi-secure and light-dangerous land will decrease 5.6% of the global land area by ~ 2100 under RCP8.5 scenario. The greatest increase in area will be in severe-dangerous regions, which will increase from 23.3% to 28.9% of the global land area by ~ 2100 under RCP8.5 scenario. By comparing the areal changes of insecure land from 2000 to 2015 to those from 2085 to 2100 under RCP8.5 scenario, the increased areas of the semi-secure, light-

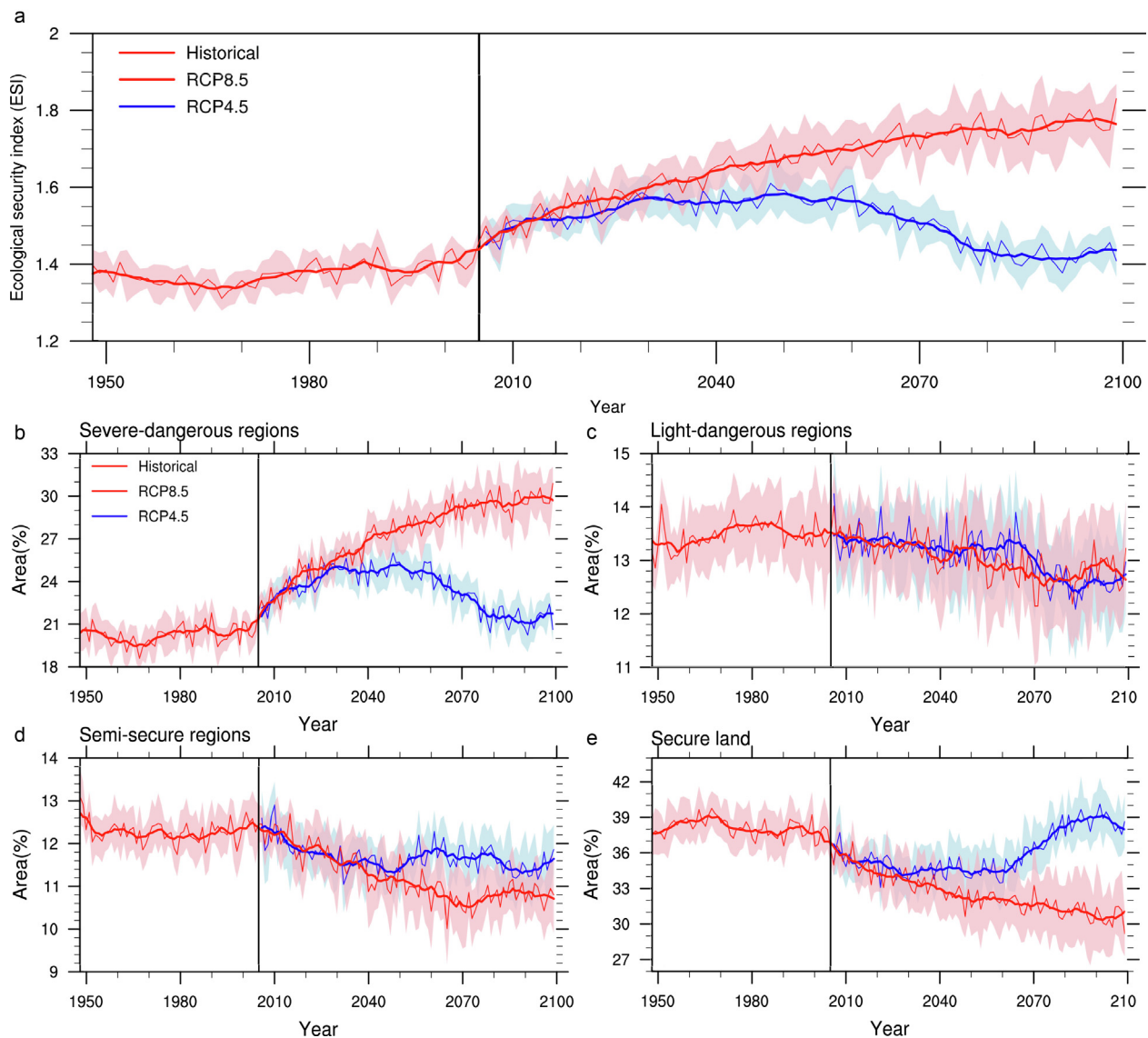


**Fig. 4.** Temporal variations in the global mean ESI and changes in the area coverage of different land surface types. a, Time series of globally averaged ESI values obtained from the CMIP5-EM. b-e, Area coverage (percentage) are shown for severe-dangerous regions (b), light-dangerous regions (c), semi-secure regions (d) and secure regions (e). The thin red (blue) solid lines are the CMIP5-EM from the historical simulations and RCP8.5 (RCP4.5) projections. The shading denotes the 95% confidence intervals of the 18 models. Seven-year running means (thick colored lines) are shown to emphasize the Earth's health trends.

dangerous and severe-dangerous regions are 4.6%, 5.6% and 7.8%, respectively, and the net areal changes of secure land and severe-dangerous regions represent  $-4.1\%$  and  $5.6\%$  of global land, respectively. The increase in severe-dangerous regions (reaching up to 28.9% of the global land area by 2100) is the most significant, which is mainly attributed to the remarkable decrease in secure land and the slight decrease in semi-secure and light-dangerous regions.

### 5. Discussion

Achieving the Sustainable Development Goals requires maintaining a balance between the environment, society and the economy. Environmental sustainability has always been an important part of sustainable development and a necessary condition for achieving strong sustainability (Wu, 2013). In order to achieve environmental sustainability, building a reasonable index can guide policymaker in the right direction. There are many indexes available for assessing environmental sustainability, such as Ecological Footprint (Wackernagel and Rees, 1996), Environmental Sustainability Index and Environmental

Performance Index (<http://sedac.ciesin.columbia.edu/es/epi/>), which are only published on the national scale. Of course, ecological security is also an important indicator. Ecological security has emerged as a critical policy focus across the world. Governments are increasingly being asked to explain their performance on a range of environment protection and natural resource management challenges with reference to quantitative metrics. Ecological security index can make us easier to spot problems, track trends, identify best practices, and optimize the gains from constructions of ecological civilization.

As the oxygen is the most important survival factor of all animals on the earth, its content directly determines the biomass of the earth. Several historical mass extinctions have been associated with reduced oxygen concentration during historical periods. In the past 100 years, under the frequent intervention of human activities, many resources on the earth have been in an over-used state, including fresh water resources, and we have crossed the threshold of one-third of the 9 planetary boundaries proposed by Rockström et al. (2009). Also, the over-exploitation and use of fossil fuels has also led to a record high rate of human oxygen consumption and carbon dioxide emissions, and its

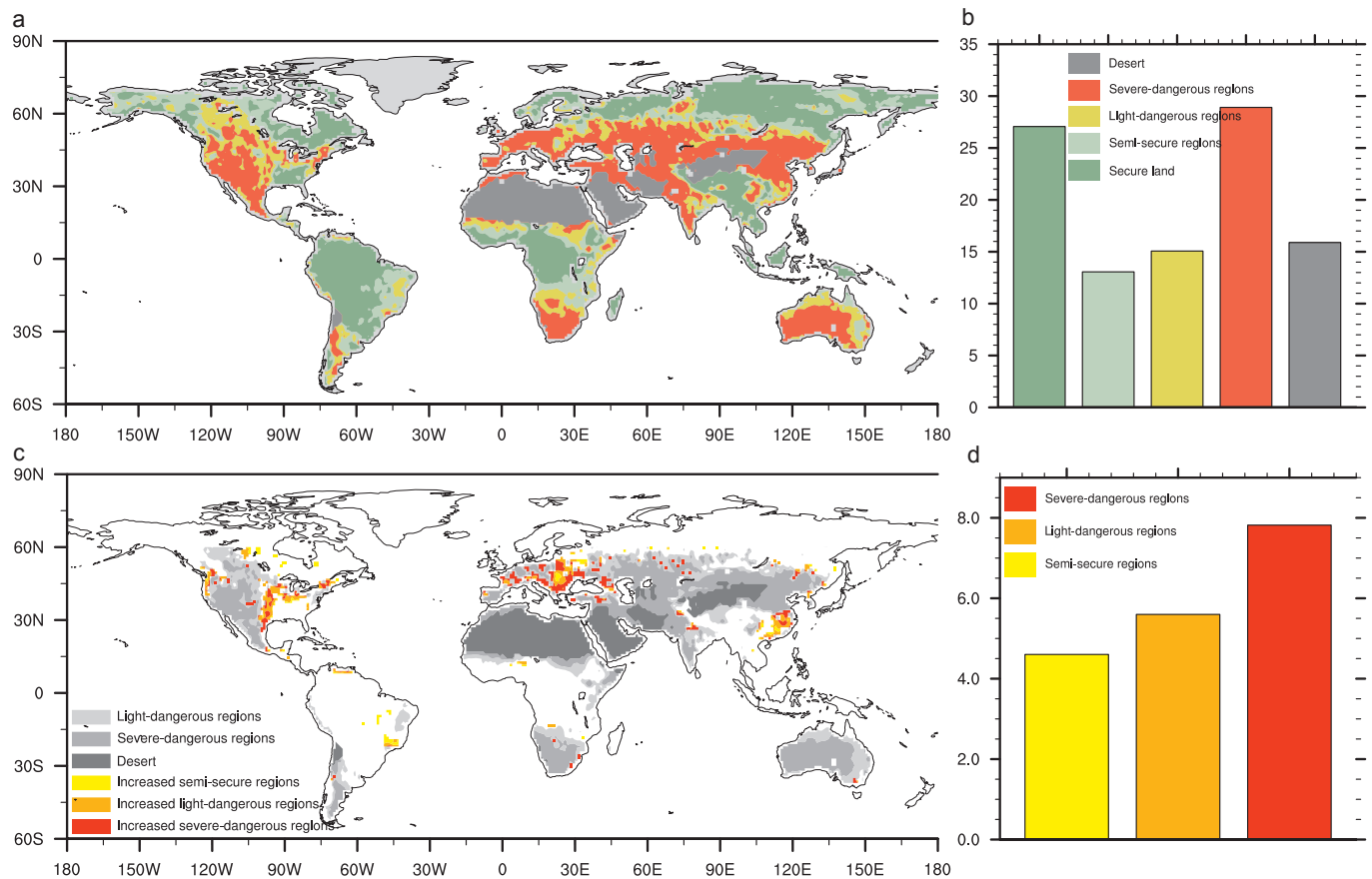


**Fig. 5.** Global distribution of ESI from CMIP5-EM and RCP8.5 scenario for 2085–2100 and its changes in relative to observations from 2000 to 2015 a, Spatial distribution of projected ESI values for 2085–2100. b, Area coverage (percentage) of different land surface types (60°S–60°N) based on projected ESI values from 2085 to 2100. c, Projections of changes in subtypes from the CMIP5-EM and RCP8.5 scenario are shown relative to the baseline period (observations, 2000–2015) for 2085–2100. The gray shading denotes the baseline land surface types from 2000 to 2015. Changes include any transitions between adjacent and nonadjacent subtypes. For example, the ‘increased’ category means that the indicated regions transitioned from more secure subtypes, i.e., the ‘increased semi-secure’ category represents regions that changed from being secure to semi-secure. d, The increased area coverage (percentage) of different land surface types (60°S–60°N) shown in c.

greenhouse effect has led to the overall warming of the earth. During the Anthropocene, due to the expansion of urban area and the acceleration of desertification, the oxygen produced by the earth’s vegetation also gradually decreased. Increased oxygen consumption and decreased oxygen production have put the planet which we live in on an unsustainable state. In this article, we combined the oxygen consumption, the oxygen production, the global warming and the extent of land aridity to construct an ESI and make future estimates.

Obviously, geoscientists can apply the newly proposed ESI to investigate and reanalyze the vitality of land with different ecological statuses, especially the formation and expansion of insecure land. The systematic classification of land using ESI can not only alert us to climate crises due to natural insecure land but can also warn us about the hidden threat from anthropogenic insecure land, which has mostly been ignored worldwide due to greed-driven human activities. Under global change, extreme weathers and human disturbances, such as rapid population growth and accelerate urbanization, have an increasing impact on the ecosystem stability. The above results highlight that when the external forcing are beyond the environmental capacity, the secure land would become unsustainable and the risk of ecological security would occur. Based on the population projections under SSP5 (RCP8.5), the global population will increase to 12.7 billion by 2100, indicating that more people will be threatened by severe ecological security. Thus, detecting the starting point of insecure land at an earlier stage and preventing its invasion is of particular importance and a high priority because it can further avoid insecure land from connecting altogether and decelerate the expected losses of biological species richness

(Pounds et al., 2006). Thus, more urgent actions must be taken to promote oxygen production and preserve water resources, including planting more trees, slowing down the expansion of deserts and drylands to stop dust from spreading (Shugart et al., 2003) and cultivating new green land among large regions of insecure land. In addition, we must avoid extra activities that consume more oxygen and water, especially by limiting fossil fuel combustion, forbidding ocean and lake trash, properly disposing of municipal and industrial waste and evenly distributing industrial zones. If we continue to take land resources for granted, more land will definitely develop into insecure land and even desert; this final step is irreversible and can cause humans to permanently lose their habitat (Prentice et al., 2007). Therefore, it is unwise and lacking in foresight to trade actual land resources for rapid economic development. We must establish new policies to stop the environment from worsening any further using global cooperation without hesitation.

**CRedit authorship contribution statement**

**Jianping Huang:** Conceptualization, Writing - original draft, Writing - review & editing, Supervision. **Haipeng Yu:** Methodology, Validation, Writing - original draft, Writing - review & editing. **Dongliang Han:** Resources, Writing - review & editing. **Guolong Zhang:** Validation, Writing - review & editing. **Yun Wei:** Methodology, Writing - review & editing. **Jiping Huang:** Formal analysis, Investigation. **Linli An:** Formal analysis, Investigation. **Xiaoyue Liu:** Data curation, Software, Visualization. **Yu Ren:** Software,

Visualization, Resources.

## Declaration of Competing Interest

The authors declare that they have no known competing financial interests or personal relationships that could have appeared to influence the work reported in this paper.

## Acknowledgments

This work was jointly supported by the National Science Foundation of China (41991231 and 41521004), the Strategic Priority Research Program of Chinese Academy of Sciences (Grant No. XDA2006010301) and the China University Research Talents Recruitment Program (111 project, No. B13045). The authors acknowledge the World Climate Research Programme's (WCRP) Working Group on Coupled Modelling (WGCM), the Global Organization for Earth System Science Portals (GO-ESSP) for producing the CMIP5 model simulations and making them available for analysis.

## Data availability

The authors declare that the data supporting the findings of this study are available within the article.

## References

- Allenby, B.R., 2000. Environmental security: concept and implementation. *Int. Polit. Sci. Rev.* 21, 5–21.
- Cai, W.J., Wan, L.Y., Jiang, Y.K., Wang, C., Lin, L., et al., 2015. Short-lived buildings in China: impacts on water, energy, and carbon emissions. *Environ. Sci. Technol.* 49, 13921–13928.
- Chen, M., Xie, P., Janowiak, J.E., et al., 2002. Global land precipitation: a 50-yr monthly analysis based on gauge observations. *J. Hydrometeorol.* 3, 249–266.
- Ciais, P., 1999. Restless carbon pools. *Nature* 398, 111–112.
- Costanza, R., Mageau, M., 1999. What is a healthy ecosystem? *Aquat. Ecol.* 33, 105–115.
- Dai, A.G., Zhao, T.B., 2017. Uncertainties in historical changes and future projections of drought. Part I: estimates of historical drought changes. *Clim. Change* 144, 519–533.
- Daly, H.E., 2005. Georgescu-roegen versus solow/stiglitz. *Ecol. Econ.* 22, 261–266.
- Dickinson, R.E., 2005. Overview: the climate system. In: Potter, T.D., Colman, B.R. (Eds.), *Handbook of Weather, Climate, and Water*. Wiley-Interscience, Manhattan, pp. 117–127.
- Fan, Y., Dool, H.V.D., 2014. Climate Prediction Center global monthly soil moisture data set at 0.5 degree resolution for 1948 to present. *J. Geophys. Res. Atmos.* 109, D10102.
- Feng, S., Fu, Q., 2013. Expansion of global drylands under a warming climate. *Atmospheric Chem. Phys.* 13, 10081–10094.
- Feng, X.M., Fu, B.J., Piao, S.L., 2016. Revegetation in China's Loess Plateau is approaching sustainable water resource limits. *Nat. Clim. Change* 6, 1019.
- Feng, Y.J., Yang, Q.Q., Tong, X.H., 2018. Evaluating land ecological security and examining its relationships with driving factors using GIS and generalized additive model. *Sci. Total Environ.* 633, 1469–1479.
- Fu, B.J., Li, Y., 2016. Bidirectional coupling between the Earth and human systems is essential for modeling sustainability. *Natl. Sci. Rev.* 3, 397–398.
- Fu, B.J., Tian, H.Q., Tao, F.L., 2017. The impact of global change on ecosystem services. *China Basic Sci.* 19, 14–18 (In Chinese).
- Fu, B.J., 2010. Trends and priority areas in ecosystem research of China. *Geogr. Res.* 29, 383–396 (In Chinese).
- Glover, J.D., Reganold, J.R., Bell, W.L., et al., 2010. Increased food and ecosystem security via perennial grains. *Science* 328, 1638.
- Harris, I., Jones, P.D., Osborn, T.J., et al., 2014. Updated high-resolution grids of monthly climatic observations—the CRU TS3.10 Dataset. *Int. J. Climatol.* 34, 623–642.
- Hodson, M., Marvin, S., 2009. 'Urban ecological security': a new urban paradigm? *Int. J. Urban Reg. Res.* 33, 193–215.
- Hu, M.M., Li, Z.T., Yuan, M.J., et al., 2019. Spatial differentiation of ecological security and differentiated management of ecological conservation in the Pearl River Delta, China. *Ecol. Ind.* 104, 439–448.
- Huang, J.P., Guan, X.D., Ji, F., 2012. Enhanced cold-season warming in semi-arid regions. *Atmos. Chem. Phys.* 12, 5391–5398.
- Huang, J.P., Huang, J.P., Liu, X.Y., et al., 2018. The global oxygen budget and its future projection. *Sci. Bull.* 63, 1180–1186.
- Huang, J.P., Ji, M.X., Xie, Y.K., et al., 2016. Global semi-arid climate change over last 60 years. *Clim. Dyn.* 46, 1131–1150.
- Huang, J.P., Xie, Y.K., Guan, X.D., et al., 2017a. The dynamics of the warming hiatus over the Northern Hemisphere. *Clim. Dyn.* 48, 429–446.
- Huang, J.P., Yu, H.P., Dai, A.G., et al., 2017b. Drylands face potential threat under 2°C global warming target. *Nat. Clim. Change* 7, 417–422.
- Huang, J.P., Yu, H.P., Guan, X.D., et al., 2015. Accelerated dryland expansion under climate change. *Nat. Clim. Change* 6, 166.
- Humphrey, V., Gudmundsson, L., Seneviratne, S.I., 2017. A global reconstruction of climate-driven subdecadal water storage variability. *Geophys. Res. Lett.* 44, 2300–2309.
- IUCN. IUCN Red List Categories and Criteria: Version 3.1. IUCN Bulletin 2012.
- Jacobson, M.C., Charlson, R.J., Rodhe, H. et al., 2000. *Earth System Science : from Biogeochemical Cycles to Global Change*. London: Academic Press.
- Jenkins, C.N., Pimm, S.L., Joppa, L.N., 2013. Global patterns of terrestrial vertebrate diversity and conservation. *Proc. Natl. Acad. Sci.* 110, E2602–E2610.
- Liu, D., Chang, Q., 2015. Ecological security research progress in China. *Acta Ecologica Sinica* 35, 111–121.
- Liu, X.Y., Huang, J.P., Huang, J.P., et al., 2020. Estimation of gridded atmospheric oxygen consumption from 1975 to 2018. *J. Meteorol. Res.* 34, 1–13.
- Ma, K.M., Fu, B.J., Li, X.Y., et al., 2004. The regional pattern for ecological security (RPES): the concept and theoretical basis. *Acta Ecologica Sinica* 04, 105–112 (In Chinese).
- Morice, C.P., Kennedy, J.J., Rayner, N.A., et al., 2012. Quantifying uncertainties in global and regional temperature change using an ensemble of observational estimates: the HadCRUT4 dataset. *J. Geophys. Res.* 117, D08101.
- Newbold, T., Hudson, L.N., Hill, S.L.L., et al., 2015. Global effects of land use on local terrestrial biodiversity. *Nature* 520, 45–50.
- Palmer, M., Bernhardt, M., Chornesky, E., et al., 2004. Ecology for a crowded planet. *Science* 304, 1251.
- Petsch, S.T., 2013. The Global Oxygen Cycle. In Heinrich, D., Holland and Karl, K. Turekian (eds.). *Treatise on Geochemistry: Second Edition*. London, Oxford: Elsevier, 437–473.
- Piao, S.L., Ciais, P., Huang, Y., et al., 2010. The impacts of climate change on water resources and agriculture in China. *Nature* 467, 43–51.
- Piao, S., Wang, X., Park, T., et al., 2020. Characteristics, drivers and feedbacks of global greening. *Nat. Rev. Earth Environ.* 1, 14–27.
- Pounds, J.A., Bustamante, M.R., Coloma, L.A., et al., 2006. Widespread amphibian extinctions from epidemic disease driven by global warming. *Nature* 439, 161–167.
- Prentice, I.C., Bondeau, A.B., Cramer, W., et al., 2007. Terrestrial ecosystems in a changing world. In: Canadell, J.G., Pataki, D., Pitelka, L.F. (Eds.), *Terrestrial Ecosystems in a Changing World*. Springer, Berlin, pp. 175–192.
- Rapport, D.J., 1989. What constitutes ecosystem health? *Perspect. Biol. Med.* 33, 120–132.
- Rockström, J., Steffen, W., Noone, K., et al., 2009. A safe operating space for humanity. *Nature* 461, 472–475.
- Schlesinger, W.H., Reynolds, J.F., Cunningham, G.L., et al., 1990. Biological feedbacks in global desertification. *Science* 247, 1043–1048.
- Seneviratne, S.I., Corti, T., Davin, E.L., et al., 2010. Investigating soil moisture-climate interactions in a changing climate: A review. *Earth Sci. Rev.* 99, 125–161.
- Shinoda, M., Yamaguchi, Y., 2003. Influence of soil moisture anomaly on temperature in the Sahel: a comparison between wet and dry decades. *J. Hydrometeorol.* 4, 437–447.
- Shugart, H., Sedjo, R., Sohngen, B., 2003. *Forests & Global Climate Change: potential impacts on U.S. forest resources*. Pew Center on Global Climate Change.
- Sohn, L.B., 1973. The Stockholm declaration on the human environment. *Harvard Int. Law J.* 14, 423–515.
- Sorooshian, S., Lawford, R.G., Try, P., et al., 2005. Water and energy cycles: investigating the links. *World Meteorol. Organ. Bull.* 54, 58–64.
- Taylor, K.E., Stouffer, R.J., Meehl, G.A., 2012. An overview of CMIP5 and the experiment design. *Bull. Am. Meteorol. Soc.* 93, 485–498.
- Van, der, Werf, G.R., Randerson, J.T., Giglio, L., et al., 2017. Global fire emissions estimates during 1997–2016. *Earth Syst. Sci. Data* 9, 697–720.
- Vörösmarty, C.J., McIntyre, P.B., Gessner, M.O., et al., 2010. Global threats to human water security and river biodiversity. *Nature* 467, 555–561.
- Wackernagel, M., Rees, W.E., 1996. *Our Ecological Footprint: Reducing Human Impact on the Earth*. New Society Publishers, British Columbia, Canada.
- Walther, G.-R., Post, E., Convey, P., et al., 2002. Ecological responses to recent climate change. *Nature* 416, 389–395.
- Wang, S.R., Meng, W., Jin, X.C., et al., 2015. Ecological security problems of the major key lakes in China. *Environ. Earth Sci.* 74, 3825–3837.
- Wu, Jianguo, 2013. Landscape sustainability science: ecosystem services and human well-being in changing landscapes. *Landscape Ecol.* 28 (6), 999–1023.
- Yang, Y.T., Roderick, M.L., Zhang, S.L., et al., 2019. Hydrologic implications of vegetation response to elevated CO<sub>2</sub> in climate projections. *Nat. Clim. Change* 9, 44–48.
- Zhao, W.W., Wei, H., Jia, L.Z., et al., 2018. Soil erodibility and its influencing factors on the Loess Plateau of China: a case study in the Ansai watershed. *Solid Earth* 9, 1507–1516.